Robotica: (2021) volume 39, pp. 1163–1180. © The Author(s), 2020. Published by Cambridge University Press.
doi:10.1017/S0263574720000971

Perfect Torque Compensation of Planar 5R Parallel Robot in Point-to-Point Motions, Optimal Control Approach

Mojtaba Riyahi Vezvari†, Amin Nikoobin†* and Ali Ghoddosian‡

†*Robotics and Control Research Laboratory, Faculty of Mechanical Engineering, Semnan University, Semnan, Iran. E-mail: mrv@semnan.ac.ir*
‡*Faculty of Mechanical Engineering, Semnan University, Semnan, Iran.*
E-mail: aghoddosian@semnan.ac.ir

(Accepted September 15, 2020. First published online: October 13, 2020)

SUMMARY
In this paper, a new approach is presented for perfect torque compensation of the robot in point-to-point motions. The proposed method is formulated as an open-loop optimal control problem. The problem is defined as optimal trajectory planning with adjustable design parameters to compensate applied torques of a planar 5R parallel robot for a given task, perfectly. To illustrate the effectiveness of the approach, the obtained optimal path is used as the reference command in the experiment. The experimental outputs show that the performance index has been reduced by over 80% compared to the typical design of the robot.

KEYWORDS: Planar 5R parallel robot; Counterweights; Point-to-point motion; Optimal trajectory; Optimal control; Torque compensation.

1. Introduction

The parallel robot is a closed-loop mechanism consisted of a closed-loop kinematic chain. The end effector of the parallel robot is connected to the ground by the kinematic chain.[1] Due to their great performance in terms of speed, rigidity, and accuracy, parallel robots have proved useful in many applications,[2] one which is pick-and-place operation. Such an operation is very common in food, electronics, and pharmaceutical industries. In the point-to-point motion, the end effector repeatedly moves between two given positions. In many practical situations, the end effector needs to move in a planar point-to-point motion. For this particular problem, the planar 5R parallel robot is introduced. Huang et al. presented a design of planar 5R parallel robot using the properties of parallelograms. This was performed by the optimal dimensional synthesis of the robot.[3] Pierrot et al. presented a new architecture known as Par2 to perform 2-Degrees of freedom (DOF) pick-and-place tasks. Par2 has two actuated kinematic chains and also two passive chains.[4] Huang et al. proposed an approach for the optimal design of planar 5R parallel robot. Considering the normalized inertial and centrifugal/Coriolis torques, two dynamic performance indices were proposed for the minimization.[5] Meng et al. proposed a novel 2-DOF translational parallel robot named as V2. Three motion/force transmission and constraint indices are introduced for V2.6 Sang et al. proposed a local performance evaluation taking into consideration the directional variation of robots' performance. A circular trajectory around a local output point is considered as a target trajectory. This approach was applied to a five-bar parallel robot.[7] Dincer and Cevik introduced a new composite polynomial in the trajectory planning of a 2-DOF parallel mechanism. This polynomial combines cubic polynomials with Bezier curves based on quadratic Bernstein polynomials.[8]

* Corresponding author. E-mail: anikoobin@semnan.ac.ir

For robotic systems, the problem of motion planning and control are divided into two levels.[9] The first level is called path or trajectory planning, and the second level is called trajectory tracking or path control. The trajectory planning often generates off-line movements to perform tasks in a defined environment.[10] The trajectory tracking is carried out in real time.[8,11] For trajectory planning problem, it is possible to find different optimality criteria; the most significant are minimum execution time, minimum effort, and minimum jerk. The criterion of minimum effort for the planar 5R parallel robot is a significant problem in the point-to-point motions. This criterion is used for minimization of torque, power, and energy of robotic manipulators.

The criterion of minimum effort has been studied in previous literature. A review of related literature shows that the minimization problem can be classified into two groups. In the first group, the mass or geometric parameters of the robot are not considered as design parameters. While in the second group, robot parameters are introduced as the design variables determined by solving the problem. Thus, these two groups are called "optimal motion generation" and "optimal redistribution of design parameters", respectively.

In the first group, trajectory planning for a specified robotic system is presented. Luo et al. used the Lagrange interpolation method for the joint angles of the robot manipulators. Using this method, an optimal trajectory was obtained for energy minimization.[12] Boscariol and Gasparetto presented a solution for constrained robust trajectory planning of nonlinear mechatronic systems. The inclusion of constraints does not affect actuator effort.[13] Kucuk developed an optimal trajectory generation algorithm for generating minimum-time smooth motion trajectories for serial and parallel manipulators. This algorithm consumes less power to perform the trajectory tracking task.[14] Bagheri et al. considered the trajectory optimization of a 7-DOF manipulator using both the heuristic- and gradient-based methods. The cost function is formulated as mechanical energy consumption with torque saturation constraints.[15] Gong et al. performed a study on the optimal control to find optimal pose at target for a planar 3-DOF manipulator. Accordingly, they reached an optimal trajectory for which the torque was minimized while dynamics were taken into consideration.[16] Nusbaum et al. considered the problem of energy minimization for a given task. The problem is formulated as a constrained optimal control to the simultaneous path planning and control optimization of redundant systems.[17] Woolfrey et al. analyzed the problem of torque minimization for a redundant serial link manipulator where an external force acts on the end effector. Using null space control, the redundant task is designed to reduce the dynamic torque.18 Boscariol and Richiedei presented a method for planning minimum energy trajectories of Cartesian robots. The trajectory for each joint of the robot was defined by spline functions.[19]

In the second group, some robot parameters are considered to be unknown, which is calculated in the problem-solving process. Quaglia and Yin proposed a method to design the spring parameters of balancing devices for articulated robots. This method produces the proper torque of the robot.[20] Nikoobin et al. presented an optimal balancing method to minimize the torque at joints of the serial robot. The method calculates states, controls, and unknown parameters of the robot for a point-to-point motion, simultaneously.[21] They developed their work for planar cable robot[22] and spatial cable robot.[23] Arakelian studied the gravity compensation methods applied in robotics. They also examined some properties of the gravity compensation and presented the results via kinematic schemes. Three principal groups are considered to classify the balancing schemes: counterweight, spring, and active force.[24] Misaghi et al. proposed an optimization method to minimize the energy consumption of a 3-DOF parallel robot by adding weights to the links. The dynamic analysis of the robot is performed by the principle of virtual work to obtain an optimal set of dynamic parameters.[25] Moradi et al. utilized a closed-loop method to find the optimal controller/parameters of an open-chain robot manipulator in point-to-point motion. The optimality conditions are derived using the closed-loop optimal control theory.[26] They developed their work for a repetitive full-cycle motion of robot manipulators including different subtasks. The entire cycle of motion is considered an optimal balancing problem.[27] Zhang et al. proposed an analytically tractable solution to gravity balancing a planar four-bar linkage. They provided an optimal generation of the balancing developed by a nonzero length spring.[28] Gupta et al. investigated optimum design of serial robotic manipulators for minimum driving torques/forces at joints. They proposed an alternate dynamic formulation based on the concept of the equimomental system of point masses and the decoupled natural orthogonal complement.[29] Martini et al. presented an approach to statically balance of open and closed kinematic

https://doi.org/10.1017/S0263574720000971 Published online by Cambridge University Press

chains. The proposed algorithm determines the balance arrangement by installing combinations of counterweights and springs.[30]

This paper uses the optimal control theory for the torque compensation problem.[31] In the optimal control, the optimality conditions are expressed as a set of differential equations based on Pontryagin's minimum principle (PMP). According to the initial condition, the optimal control can obtain the exact solution of the problem. This method has been widely used for analyzing nonlinear systems and trajectory planning for different types of system.[32–34] Korayem et al. presented a trajectory optimization for a non-holonomic mobile manipulator in pursuing a moving target. The dynamic motion planning of the system is formulated as an optimal control problem.[35] Rahaghi and Barat investigated the dynamic load carrying capacity of a manipulator in the specified path. They used a new closed-loop optimal control method.[36] In these studies, the performance index was minimized or maximized rather than obtaining a global optimum response. Also, the adjustable design parameters for the system are not considered in the optimization problem.

The main purpose of the above studies is to reduce the torque or power consumption. Among them, static balancing or gravity compensation methods can be a simple and effective approach for the low-speed tasks. But, its efficiency is reduced due to the increase in inertial forces in the high-speed operations. Each of the previous methods has provided a solution to reduce power, but none has reached zero. In this paper, a new approach is presented for perfect torque compensation of the robotic systems in point-to-point motion. For a predefined point-to-point task, the proposed method is formulated as an optimal control problem,[31] in which the design parameters of the robot and the optimal trajectories are calculated simultaneously in order to compensate the applied torques at joints. The mass of the counterweights and the installation angle of them, with reference to the robot links, are considered as design parameters. The both mass and angle of the counterweights are determined by solving the optimal control problem.

In the proposed method, the counterweights parameters are determined off-line for a given boundary condition and the given time interval. The presented approach is suitable for a situation in which the start and end points are fixed or have little change. The method is applied to a planar 5R parallel robot with the adjustable counterweights.

This paper is organized in five sections. In Section 2, formulation of the perfect torque compensation method (PTCM) is presented and the dynamic equations for a planar 5R parallel robot are derived considering the counterweights. Section 3 illustrates the effectiveness of the proposed method to cause a swinging motion, with zero torque, between the two given points in the task space via theoretical simulation. In order to verify the PTCM, experimentations are carried out, the results of which are presented in the fourth section. Finally, Section 5 draws conclusions from this study.

2. Formulation of PTCM

In this section, a new approach for torque minimization problem called PTCM is introduced for the planar 5R parallel robot. The optimal control theory is used to achieve the necessary conditions for the implementation of PTCM. The necessary conditions are expressed as a set of differential equations based on PMP. In the proposed approach, the trajectory of the robot, unknown parameters of counterweights, and the performance index are calculated simultaneously for a point-to-point motion.

2.1. Dynamic modeling of planar 5R parallel robot with counterweights

A kinematic scheme of the robot with counterweights is shown in Fig. 1, in which two counterweights were attached to the links 1 and 3. This arrangement for two adjustable counterweights is a design choice. This choice simplifies the practical implementation of the planar 5R parallel robot. In here, m_{ci}, r_{ci}, and $\alpha_{ci} (i = 1, 2)$ are mass, length, and installation angle of the ith counterweight with reference to the link $2i$-1.The moment of inertia of the counterweights is ignored and they are considered as point masses.

The kinematic model of the robot can be simplified as a planar five-bar mechanism. The position of point P is

$$\begin{cases} x_p = A_i + l_{2i-1}\, cos\theta_i + l_{2i}\, cos\beta_i \\ y_p = l_{2i-1}\, sin\theta_i + l_{2i}\, sin\beta_i \end{cases} ;\ i = 1, 2, \tag{1}$$

https://doi.org/10.1017/S0263574720000971 Published online by Cambridge University Press

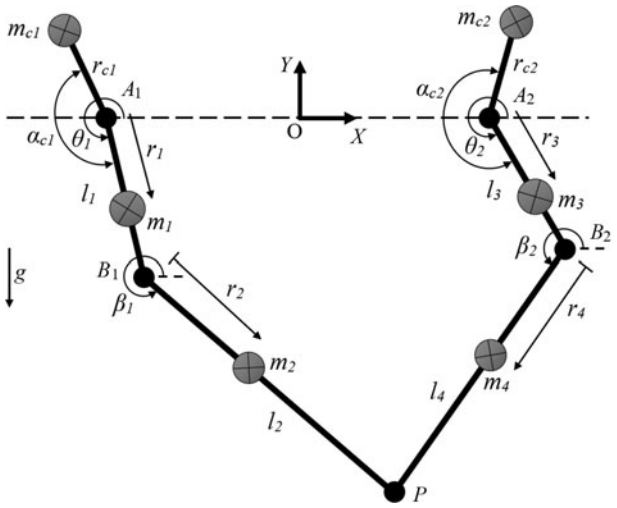

Fig. 1. A kinematic scheme of considered planar 5R parallel robot with counterweights.

where l_{2i-1} and l_{2i} are the length of the proximal and distal links; A_i is the offset from coordinate system XOY; θ_i and β_i are the angular positions of the proximal and distal links, respectively.

The active joint angles $\theta_i (i = 1, 2)$ and the angular velocities $\dot{\theta}_i (i = 1, 2)$ are obtained by Eqs. (2) and (3), respectively:[5,37]

$$\theta_i = 2\, tan^{-1}\left(\frac{-D_i + sgn\,(j)\sqrt{D_i^2 + E_i^2 - F_i^2}}{F_i - E_i}\right); i = 1, 2,\ sgn\,(j) = \begin{cases} 1 & j = 1 \\ -1 & j = 2 \end{cases} \tag{2}$$

$$D_i = -2l_{2i-1}y_p,\quad E_i = 2l_{2i-1}\left(A_i - x_p\right),\quad F_i = x_p^2 + y_p^2 + A_i^2 + l_{2i-1}^2 - l_{2i}^2 - 2x_p A_i$$

$$\dot{\theta}_i = J_i \dot{X}_p;\ i = 1, 2, \tag{3}$$

where $J_i;\ i = 1, 2$ is the Jacobian matrix. The dynamic model of the robot can be obtained by Lagrange–Euler formulation. For the planar 5R parallel robot, the generalized coordinate and generalized forces of the Lagrange–Euler formulation are defined as:

$$q = X_p = \left[x_p\ y_p\right]^T,\quad Q = \tau = \left[\tau_1\ \tau_2\right]^T, \tag{4}$$

where X_p is the position of the end effector p. The term τ is the applied torque at the active joints A_1 and A_2. To calculate the kinetic and potential energies of the robot, the following steps are performed. Initially, the positions of the center of masses are determined in the global coordinate system as Eq. (5). The parameter of r demonstrates the location of the center of mass on each link:

$$\begin{aligned} x_{2i-1}^r &= A_i + r_{2i-1}\, cos\theta_i,\quad y_{2i-1}^r = r_{2i-1}\, sin\theta_i;\ i = 1, 2 \\ x_{2i}^r &= A_i + l_{2i-1}\, cos\theta_i + r_{2i}\, cos\beta_i,\quad y_{2i}^r = l_{2i-1}\, sin\theta_i + r_{2i}\, sin\beta_i;\ i = 1, 2 \\ x_i^c &= A_i + r_{ci}\cos\left(\theta_i - \alpha_{ci}\right),\quad y_i^c = r_{ci}\, sin\,(\theta_i - \alpha_{ci});\ i = 1, 2 \end{aligned} \tag{5}$$

In Eq. (5), x_{2i-1}^r and y_{2i-1}^r $(i = 1, 2)$ are the coordinates of the center of mass in link $2i$-1 in the directions of X and Y, respectively; x_{2i}^r and y_{2i}^r $(i = 1, 2)$ are the coordinates of the center of mass in link $2i$ in the directions of X and Y, respectively. Also, x_i^c and y_i^c $(i = 1, 2)$ are the coordinates of the mass of the counterweight i in the directions X and Y, respectively. By taking derivative of the above equations with respect to time, velocities of the centers of mass are obtained as:

$$\begin{aligned} \dot{x}_{2i-1}^r &= -r_{2i-1}\dot{\theta}_i\, sin\theta_i,\ \dot{y}_{2i-1}^r = r_{2i-1}\dot{\theta}_i\, cos\theta_i;\ i = 1, 2 \\ \dot{x}_{2i}^r &= -l_{2i-1}\dot{\theta}_i\, sin\theta_i - r_{2i}\dot{\beta}_i\, sin\beta_i,\ \dot{y}_{2i}^r = l_{2i-1}\dot{\theta}_i\, cos\theta_i + r_{2i}\dot{\beta}_i\, cos\beta_i;\ i = 1, 2 \\ \dot{x}_i^c &= -r_{ci}\dot{\theta}_i \sin\left(\theta_i - \alpha_{ci}\right),\ \dot{y}_i^c = r_{ci}\dot{\theta}_i\, cos\,(\theta_i - \alpha_{ci});\ i = 1, 2 \end{aligned} \tag{6}$$

https://doi.org/10.1017/S0263574720000971 Published online by Cambridge University Press

Finally, the kinetic and potential energies of the robot are determined as:

$$\begin{aligned}
&K = k + k_c, \quad U = u + u_c \\
&k = 0.5 \sum_{i=1}^{2} \left(m_{2i-1} v_{2i-1}^2 + I_{2i-1} \dot{\theta}_i^2 + m_{2i} v_{2i}^2 + I_{2i} \dot{\beta}_i^2 \right), \quad k_c = 0.5 \sum_{i=1}^{2} m_{ci} v_{ci}^2 \\
&v_{2i-1}^2 = r_{2i-1}^2 \dot{\theta}_i^2, \; v_{2i}^2 = l_{2i-1}^2 \dot{\theta}_i^2 + r_{2i}^2 \dot{\beta}_i^2 + 2 l_{2i-1} r_{2i} \dot{\theta}_i \dot{\beta}_i \, cos\,(\theta_i - \beta_i) \\
&v_{ci}^2 = r_{ci}^2 \dot{\theta}_i^2; \; i = 1, 2 \\
&u = \sum_{i=1}^{2} (m_{2i-1} \, g \, r_{2i-1} \, sin\theta_i + m_{2i} \, g \, (l_{2i-1} \, sin\theta_i + r_{2i} \, sin\beta_i)), \\
&u_c = \sum_{i=1}^{2} m_{ci} \, g \, r_{ci} \, sin\,(\theta_i - \alpha_{ci}),
\end{aligned} \tag{7}$$

where k and u are the kinetic and potential energies of the proximal and distal links of the robot, respectively; and k_c and u_c are the kinetic and potential energies of the two counterweights of the robot, respectively. Using the Lagrange–Euler formulation, the final dynamic equation of the robot is obtained as in the form of:

$$M \ddot{X}_p + N + G = J^T \tau; \quad \ddot{X}_p = \left[\ddot{x}_p \; \ddot{y}_p \right]^T, \; \tau = \left[\tau_1 \; \tau_2 \right]^T, \tag{8}$$

where M, N, and G are the matrices of inertia, Coriolis and centrifugal, and gravity terms, respectively. J is the Jacobian matrix.

For static balancing, the linear momentum formulation is used for the planar 5R parallel robot.[38] The static balancing of the robot needs a third counterweight. This counterweight is attached to the joint B_1. The mass, length, and installation angle of the third counterweight are m_{c3}, r_{c3}, and α_{c3} with reference to the link 2. The linear momentum of the system is defined as:

$$\begin{aligned}
L_o = &\left(m_1 r_1 + m_2 l_1 + \frac{m_4 r_4 l_1}{l_4} + m_{c1} r_{c1} \, e^{-i\alpha_{c1}} + m_{c3} l_1 \right) \left(i \dot{\theta}_1 \right) e^{i\theta_1} \\
&+ \left(m_3 r_3 + m_4 l_3 - \frac{m_4 r_4 l_3}{l_4} + m_{c2} r_{c2} \, e^{-i\alpha_{c2}} \right) \left(i \dot{\theta}_2 \right) e^{i\theta_2} \\
&+ \left(m_2 r_2 + \frac{m_4 r_4 l_2}{l_4} + m_{c3} r_{c3} \, e^{-i\alpha_{c3}} \right) \left(i \dot{\beta}_1 \right) e^{i\beta_1}.
\end{aligned} \tag{9}$$

To obtain the zero linear momentum, the coefficients of angular velocities become zero. Thus, the following conditions are derived as:

$$\begin{aligned}
&m_1 r_1 + m_2 l_1 + \frac{m_4 r_4 l_1}{l_4} + m_{c1} r_{c1} \, cos\alpha_{c1} + m_{c3} l_1 = 0, \quad m_{c1} r_{c1} \, sin\alpha_{c1} = 0 \\
&m_3 r_3 + m_4 l_3 - \frac{m_4 r_4 l_3}{l_4} + m_{c2} r_{c2} \, cos\alpha_{c2} = 0, \quad m_{c2} r_{c2} \, sin\alpha_{c2} = 0 \\
&m_2 r_2 + \frac{m_4 r_4 l_2}{l_4} + m_{c3} r_{c3} \, cos\alpha_{c3} = 0, \quad m_{c3} r_{c3} \, sin\alpha_{c3} = 0.
\end{aligned} \tag{10}$$

By simplification of the above equation, the specifications of counterweights are obtained by Eq. (11):

$$\begin{aligned}
&\alpha_{c1} = \alpha_{c2} = \alpha_{c3} = \pi \\
&m_{c1} = \frac{m_1 r_1 + m_2 l_1 + m_{c3} l_1}{r_{c1}} + \frac{m_4 r_4 l_1}{r_{c1} l_4}, \quad m_{c2} = \frac{m_3 r_3 + m_4 l_3}{r_{c2}} - \frac{m_4 r_4 l_3}{r_{c2} l_4}, \\
&m_{c3} = \frac{m_2 r_2}{r_{c3}} + \frac{m_4 r_4 l_2}{r_{c3} l_4}
\end{aligned} \tag{11}$$

https://doi.org/10.1017/S0263574720000971 Published online by Cambridge University Press

2.2. PTCM methodology

In this section, the implementation of the PTCM for the planar 5R parallel robot is presented. The PTCM is formulated as the optimal control problem by defining the state vector as:

$$x = \left[q^T \ \dot{q}^T \right]^T \xrightarrow{q=[x_p \quad y_p]^T,\ \dot{q}=[\dot{x}_p \quad \dot{y}_p]^T} x = \left[x_p \ y_p \ \ \dot{x}_p \ \dot{y}_p \right]^T. \tag{12}$$

By rewriting the above equation, the final form of the state vector x is obtained as:

$$x = \left[x_p \ y_p \ \ \dot{x}_p \ \dot{y}_p \right]^T \xrightarrow{x_1=x_p,\ \ x_2=y_p,\ \ x_3=\dot{x}_p,\ \ x_4=\dot{y}_p} x = \left[x_1 \ x_2 \ \ x_3 \ x_4 \right]^T. \tag{13}$$

Therefore, the dynamic Eq. (8) can be rewritten in the state-space form of:

$$f = \dot{x} \xrightarrow{\dot{x}=\left[\dot{x}_p \ \dot{y}_p \ \ \ddot{x}_p \ \ddot{y}_p \right]^T} f = \begin{bmatrix} x_3 \\ x_4 \\ M_{2\times 2}^{-1}\left(x_1, x_2, b\right)\left[J^T\tau - N\left(x, b\right) - G\left(x_1, x_2, b\right)\right]_{2\times 1} \end{bmatrix}, \tag{14}$$

where b is the vector of design parameters, which contains the unknown constant parameters of the model. Then, Hamiltonian function is defined as [36]:

$$H = L + \psi^T f, \tag{15}$$

where ψ is the co-state vector and L is the integrand of the performance index. For the planar 5R parallel robot, the control effort vector and the time interval are $u = [\tau_1 \ \ \tau_2]^T$ and $t = [0 \ \ t_f]$, respectively. By defining the performance index as the following minimum effort:

$$J = \int_0^{t_f} L \, dt = \int_0^{t_f} \left(\tau_1^2 + \tau_2^2\right) \, dt, \tag{16}$$

and the co-state vector:

$$\psi = \left[\psi_1^T \ \ \psi_2^T \right]^T \xrightarrow{\psi_1 = \left[x_5 \ x_6 \right]^T,\ \psi_2 = \left[x_7 \ x_8 \right]^T} \psi = \left[x_5 \ x_6 \ \ x_7 \ x_8 \right]^T, \tag{17}$$

the Hamiltonian function becomes

$$\begin{aligned} H = {} & \left(\tau_1^2 + \tau_2^2\right) + x_5 x_3 + x_6 x_4 \\ & + \left[x_7 \ x_8 \right]\left[M_{2\times 2}^{-1}\left(x_1, x_2, b\right)\left[J^T\tau - N\left(x, b\right) - G\left(x_1, x_2, b\right)\right]_{2\times 1}\right]_{2\times 1}. \end{aligned} \tag{18}$$

The value of J is placed between zero and positive infinity. Thus, the global optimal value of the performance index is zero.

Using the PMP, the optimality conditions are given by:

$$\dot{x} = H_\psi = \left[\frac{\partial H}{\partial \psi_1} \ \ \frac{\partial H}{\partial \psi_2} \right]^T \ \rightarrow \ \dot{x} = f, \tag{19}$$

$$\dot{\psi} = -H_x \ \rightarrow \ \ \dot{\psi} = \left[\dot{x}_5 \ \dot{x}_6 \ \ \dot{x}_7 \ \dot{x}_8 \right]^T = -\left[\frac{\partial H}{\partial x_1} \ \frac{\partial H}{\partial x_2} \ \ \frac{\partial H}{\partial x_3} \ \frac{\partial H}{\partial x_4} \right]^T, \tag{20}$$

$$H_u = 0 \ \rightarrow \ \ \frac{\partial H}{\partial \tau_1} = 0, \ \ \frac{\partial H}{\partial \tau_2} = 0, \tag{21}$$

subject to the following boundary conditions:

$$\begin{aligned} & x(0) = x_0, \ \ x(t_f) = x_f; \\ & x(0) = [\, x_1(0) \quad x_2(0) \quad x_3(0) \quad x_4(0) \,]^T = [\, x_{p0} \quad y_{p0} \quad 0 \quad 0 \,]^T, \\ & x(t_f) = [\, x_1(t_f) \quad x_2(t_f) \quad x_3(t_f) \quad x_4(t_f) \,]^T = [\, x_{pf} \quad y_{pf} \quad 0 \quad 0 \,]^T. \end{aligned} \tag{22}$$

https://doi.org/10.1017/S0263574720000971 Published online by Cambridge University Press

Table I. Parameters of examined planar 5R parallel robot.

Parameter	**Value**
Mass (kg)	$m_1 = 0.2061$, $m_3 = m_1$, $m_2 = 0.1497$, $m_4 = m_2$, $m_{c1} = 0.1$, $m_{c2} = 0.1$
Length (m)	$l_1 = 0.1171$, $l_3 = l_1$, $l_2 = 0.2452$, $l_4 = l_2$
Position of the active joints (m)	$A_1 = -0.06$, $A_2 = -A_1$
Position of the center of mass (m)	$r_1 = 0.0508$, $r_3 = r_1$, $r_2 = 0.1316$, $r_4 = r_2$, $r_{c1} = 0.07$, $r_{c2} = 0.07$
Moment of inertia (kg.m^2)	$I_1 = 0.0006$, $I_3 = I_1$, $I_2 = 0.0013$, $I_4 = I_2$
Installation angle of counterweight (rad)	$\alpha_{c1} = \pi$, $\alpha_{c2} = \pi$
Gravitational acceleration (m/s^2)	$g = 9.81$

In the above equation, $[x_{p0},\ y_{p0}]$ is the initial position at $t = 0$ and $[x_{pf},\ y_{pf}]$ is the final position at $t = t_f$. For the point-to-point motion, the initial and final velocities are set to zero, that is, $\dot{x}_{p0} = \dot{y}_{p0} = \dot{x}_{pf} = \dot{y}_{pf} = 0$.

In the PTCM, the optimal values of the design parameters are obtained by defining new state variables in the optimal control problem. Indeed, the optimal trajectory planning is implemented based on the unknown parameters of the robot. Therefore, the values of parameters depend on the dynamic equation, the performance index, and the boundary conditions of the model.

The PTCM can be performed by two groups of parameters: $[m_{c1}\ m_{c2}\ \alpha_{c1}\ \alpha_{c2}]$ or $[r_{c1}\ r_{c2}\ \alpha_{c1}\ \alpha_{c2}]$. The parameters of the first group simplify the practical implementation of the planar 5R parallel robot. Adjusting the mass of the counterweights is very simpler than adjusting their length in the experimental setup. Thus, for the planar 5R parallel robot, parameters m_{c1}, m_{c2}, α_{c1}, and α_{c2} are taken as unknown variables of the counterweights. Thus, by considering the vector of parameters:

$$b = \left[\ m_{c1}\ m_{c2}\ \ \alpha_{c1}\ \alpha_{c2}\ \right], \tag{23}$$

the new state vector μ is defined as:

$$\mu = \left[\ x_9\ x_{10}\ \ x_{11}\ x_{12}\ \right]^T. \tag{24}$$

The optimality and boundary conditions associated with the vector μ are obtained as follows:

$$\dot{\mu} = -H_b \ \rightarrow\ \ \dot{x}_9 = -\frac{\partial H}{\partial m_{c1}},\ \dot{x}_{10} = -\frac{\partial H}{\partial m_{c2}},\ \dot{x}_{11} = -\frac{\partial H}{\partial \alpha_{c1}},\ \dot{x}_{12} = -\frac{\partial H}{\partial \alpha_{c2}} \tag{25}$$

$$\mu\ (t_0) = \mu\left(t_f\right) = 0$$

$$x_9\ (0) = x_{10}\ (0) = x_{11}\ (0) = x_{12}\ (0) = x_9\left(t_f\right) = x_{10}\left(t_f\right) = x_{11}\left(t_f\right) = x_{12}\left(t_f\right) = 0. \tag{26}$$

Finally, by substituting τ_1 and τ_2 from Eq. (21) into Eqs. (19), (20), and (25), 12 nonlinear ordinary differential equations are derived, which beside the 16 boundary conditions given in Eqs. (22) and (26), form a two-point boundary value problem (TPBVP). This TPBVP is solved using the bvp4c command of MATLAB software to determine the state vector x, co-state vector ψ, new state vector μ, and the vector b.

Note that the PTCM is presented to perfect torque compensation of the robot for a predefined point-to-point task. Thus, by changing condition of motion, the problem must be resolved again and new optimal parameters are obtained. Then, the new parameters of the counterweights are adjusted and fixed on the robot. Indeed, it is not possible to change the counterweights while the robot is moving.

3. Simulation

In this section, the results of simulating the planar 5R parallel robot shown in Fig. 1 are presented. The design of planar 5R parallel robot is considered as a mirror symmetry geometry. Two cases are considered for this purpose: typical form (TF) and PTCM of the planar 5R parallel robot. In the TF case, the planar 5R parallel robot is considered without counterweights, that is, $mc_1 = mc_2 = 0$. The experimental setup presented in Section 4 is based on the robot parameter values given in Table I.

https://doi.org/10.1017/S0263574720000971 Published online by Cambridge University Press

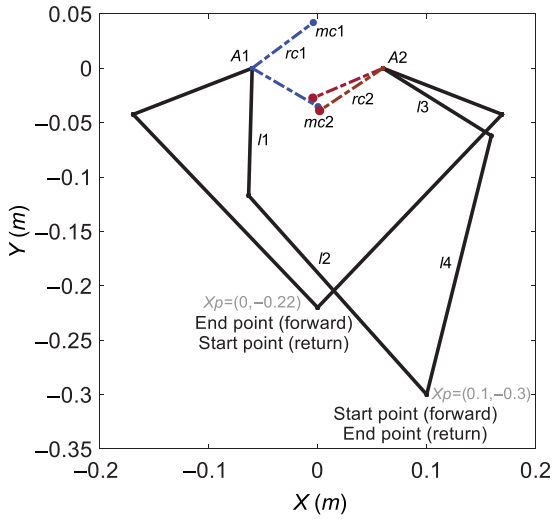

Fig. 2. Start and end positions of robot.

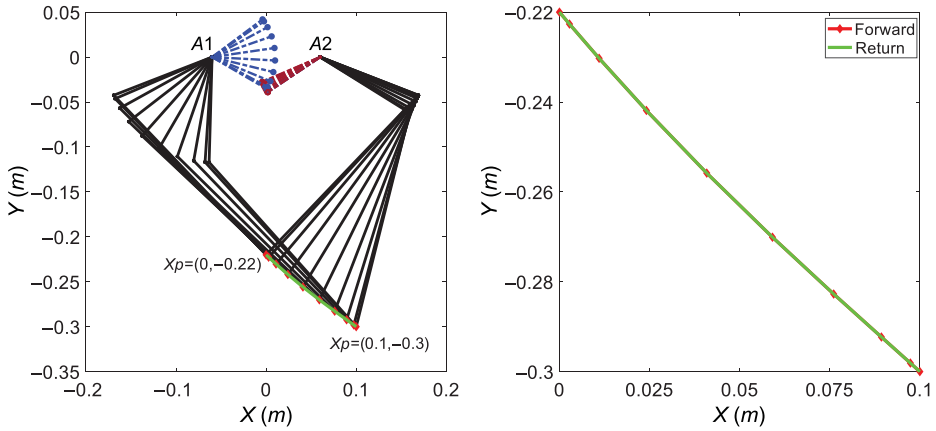

Fig. 3. Optimal trajectory of robot.

Consider a repetitive point-to-point motion with the following boundary conditions for the forward motion:

$$x_1(0) = 0.1, \quad x_2(0) = -0.3, \quad x_1(t_f) = 0, \quad x_2(t_f) = -0.22$$
$$x_3(0) = x_3(t_f) = x_4(0) = x_4(t_f) = 0, \quad t_f = 0.5 \text{ s}, \tag{27}$$

and the following boundary conditions for the return motion:

$$x_1(0) = 0, \quad x_2(0) = -0.22, \quad x_1(t_f) = 0.1, \quad x_2(t_f) = -0.3$$
$$x_3(0) = x_3(t_f) = x_4(0) = x_4(t_f) = 0, \quad t_f = 0.5 \text{ s}. \tag{28}$$

By solving the TPBVP obtained in Section 2.2, the position and velocity of the end effector and the values of m_{c1}, m_{c2}, α_{c1}, and α_{c2} of the counterweights can be computed. The start and end positions of the planar 5R parallel robot with the counterweights are shown in Fig. 2. For the forward motion, the end effector of the robot moves from [0.1 −0.3] to [0 −0.22]. In the return motion, the end effector of the robot goes from [0 −0.22] to [0.1 −0.3]. The optimal trajectories of the robot for the forward and return motions are plotted in Fig. 3. In the figure, the red and green curves show the forward and return motions of the end effector, respectively. As seen in Fig. 3, the trajectory of the end effector in the forward motion is in accordance with the trajectory of the end effector in the return motion. The position and velocity of the point p of the robot for the forward and return motions are illustrated in Figs. 4 and 5, respectively.

https://doi.org/10.1017/S0263574720000971 Published online by Cambridge University Press

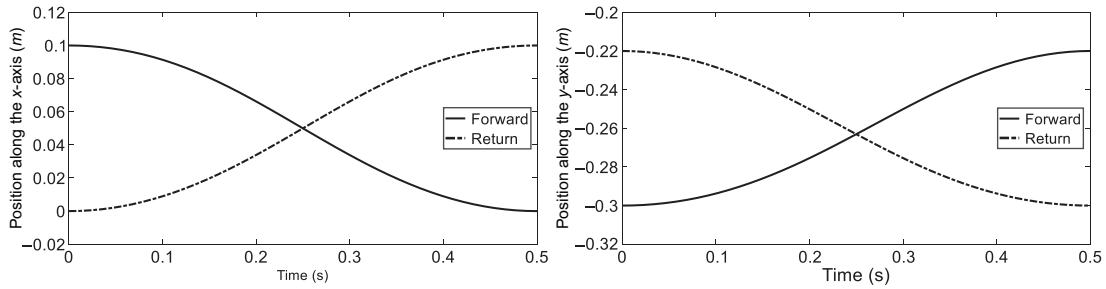

Fig. 4. Position of point *p*.

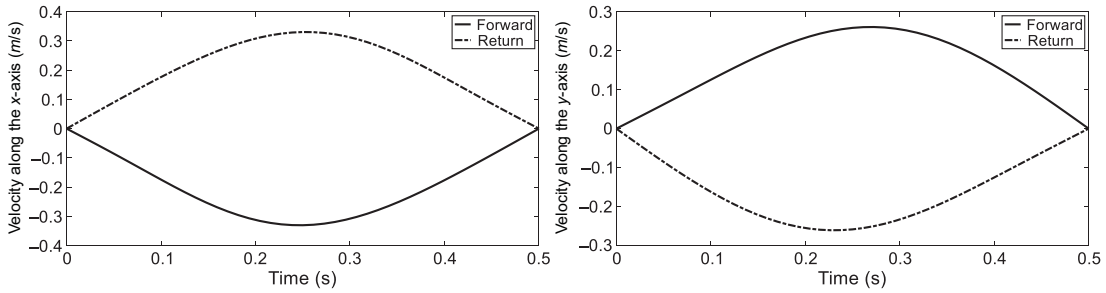

Fig. 5. Velocity of point *p*.

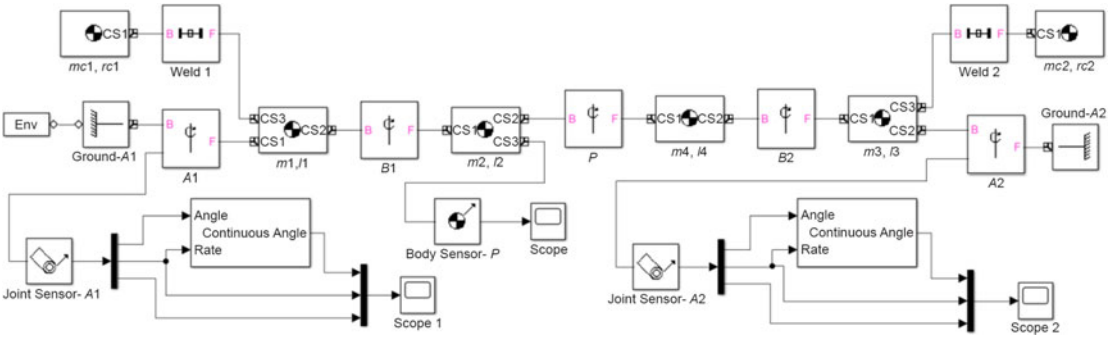

Fig. 6. Simulation of planar 5R parallel robot via SimMechanics toolbox.

As seen in Fig. 4, in the forward motion, position x of the point p moves from 0.1 to 0 m, while position y moves from –0.3 to –0.22 m. Then, in the return motion, position x of the point p returns from 0 m to 0.1 m, and position y goes back from -0.22 to -0.3 m. The time interval for both the forward and return motions is 0.5 s, making up a full-cycle period of 1 s. As shown in Fig. 5, in the both forward and return motions, the zero velocity is expected at the both start and end points.

Two interesting points are observed in the simulation results. First, for the forward and return motions, the same values of parameters are obtained: $m_{c1} = 285.1065$ g, $m_{c2} = 500.9559$ g, $\alpha_{c1} = 231.5737^{\text{o}}$, and $\alpha_{c2} = 124.8787^{\text{o}}$. Second, the torques applied on the joints A_1 and A_2 were found to be zero. Thus, it can be concluded that by properly setting the unknown parameters of the counterweights, the robot exhibits a free oscillatory motion between the start and end points. Note that the zero torque is obtained at the ideal condition without considering any friction, disturbance, and parameter uncertainty. Also, a motion without any pause at the start and end points is considered. Indeed, the PTCM is suitable for a single task in which start and end points are fixed.

Block diagram of the planar 5R parallel robot shown in Fig. 1 is created via SimMechanics toolbox to verify the results. Figure 6 presents the block diagram of the robot. The obtained parameters of counterweights and the initial conditions given in Eq. (27) are applied to the SimMechanics model. SimMechanics model of the planar 5R parallel robot is shown in Fig. 7. The model is an open-loop scheme without a controller. The position and velocity of point p computed from SimMechanics toolbox for four motion cycles are shown in Figs. 8 and 9, respectively. In Figs. 8 and 9, the robot

https://doi.org/10.1017/S0263574720000971 Published online by Cambridge University Press

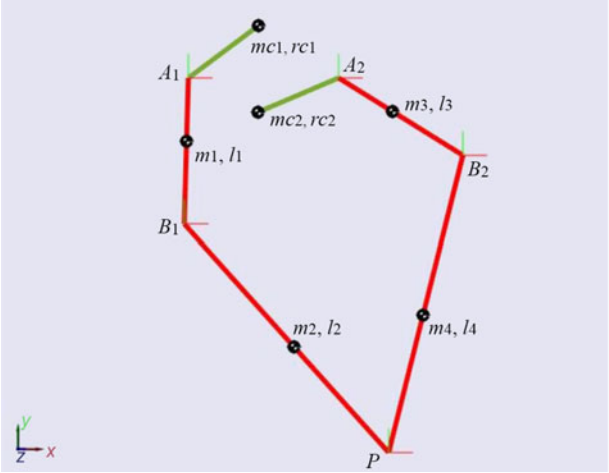

Fig. 7. SimMechanics model of planar 5R parallel robot.

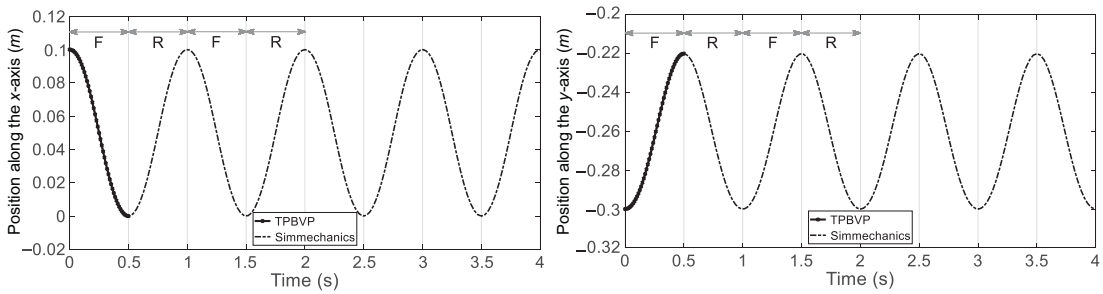

Fig. 8. Positionof point *p* obtained from SimMechanics toolbox and TPBVP.

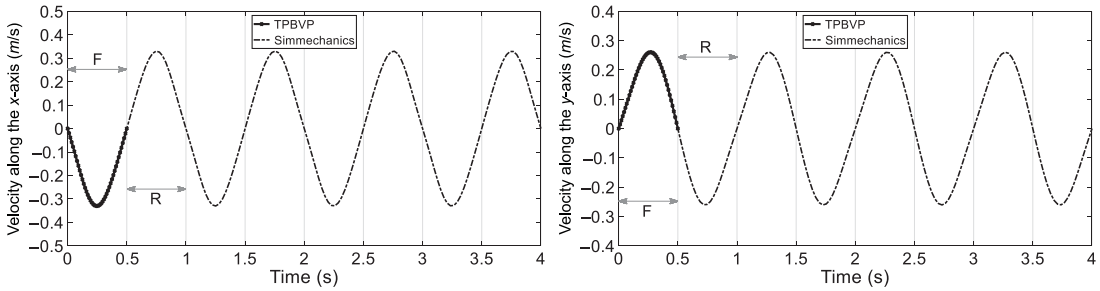

Fig. 9. Velocity of point *p* obtained from SimMechanics toolbox and TPBVP.
F: Forward, R: Return.

exhibits a free periodic motion at a period of 1 s between the start position [0.1 −0.3] and end position [0 −0.22]. Additionally, for the time interval of 0–0.5 s, the obtained results of the SimMechanics model are well in accordance with the optimal trajectory obtained from TPBVP (Figs. 4 and 5).

4. Experimental Results

In this section, the results of simulations and experiments performed for different point-to-point motions are given. For both TF and PTCM cases, the theoretical results are compared to the experimental data.

4.1. Experimental setup

For the purpose of experimentation, a planar 5R parallel robot with adjustable counterweights was designed in Semnan Robotics Lab. The robot with the counterweights is shown in Fig. 10. A graded plate is used to adjust the counterweight arm angle (Fig. 11). Figure 12 presents the parts of a counterweight.

https://doi.org/10.1017/S0263574720000971 Published online by Cambridge University Press

Table II. The experimental equipment to operate system.

Equipment	**Type**
Power supply	SMPS 12*v* and SMPS2Dynamixel
PC operating system	Windows
Connection between PC and Dynamixel	USB2Dynamixel
Compatible software with Dynamixel	Microsoft Visual Studio

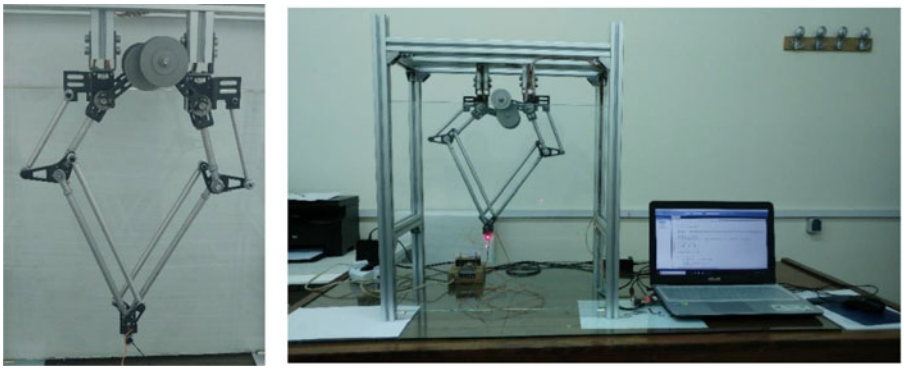

Fig. 10. Planar 5R parallel robot with two adjustable counterweights.

Fig. 11. Graded circular plate.

Counterweight arm Counterweight mass

Fig. 12. Different components of counterweight.

The servo-actuators used in the robot are Dynamixel XH430-W210 by Robotis©. The servo-actuators are operated in position control mode. This mode is ideal for articulated robots. The resolution of the actuator is 0.088 *deg*. The control algorithm of the servo-actuator is Proportional Integral Derivative (PID) control. The position sensor is a contactless absolute encoder. The current feedback is used to measure the motor torque. The torque is proportional to the motor current, so by multiplying the measured current at the motor torque constant, that is, 1.25, the applied torque can be obtained. The experimental equipment of the system is given in Table II.

The servo-actuators are operated directly from PC by USB2Dynamixel connector as shown in Fig. 13. The USB2Dynamixel is connected to USB port of PC. The Microsoft Visual Studio is used to send and receive real-time data. The programming language is C#.

Due to the friction and parametric uncertainties, it is practically impossible to implement a motion repeatedly without consuming any torque as an open-loop approach to exactly reproduce the periodic motion discussed in the previous section. Parameter uncertainties are caused by measurement error of mass, length, moment of inertia, and the position of the center of mass. Indeed, the used parameters in the simulation study are not identical to the actual values of the experimental model. Thus, two servo-actuators are used in the experimental setup to track the optimal trajectory in a closed-loop approach. The flowchart of the command diagram is shown in Fig. 14.

https://doi.org/10.1017/S0263574720000971 Published online by Cambridge University Press

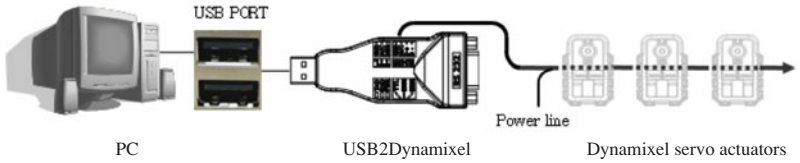

Fig. 13. Dynamixel control using PC.

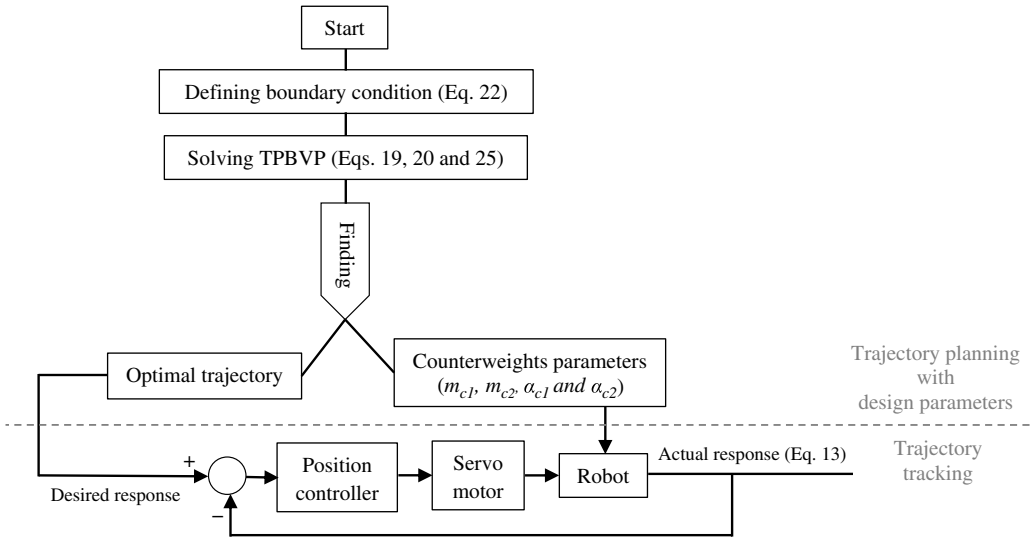

Fig. 14. Command diagram of experiment setup.

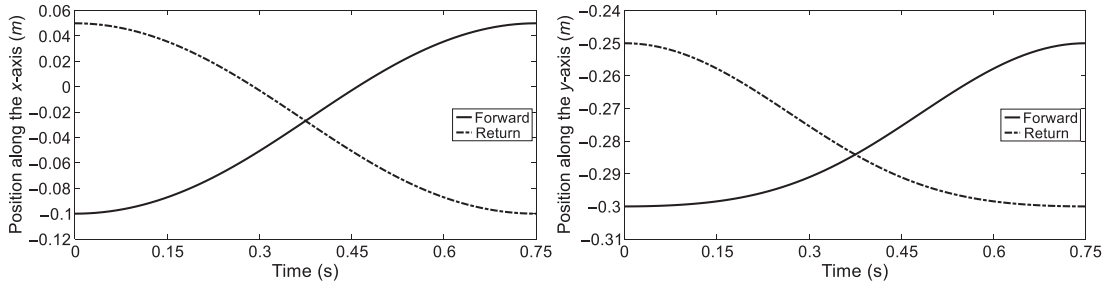

Fig. 15. Position of point p for case 2.

4.2. Examples

In this experiment, PTCM was implemented for different pairs of start and end points. Four configurations were considered (Eq. (29)) with different positions in the coordinate system *XOY*. For all cases, the velocity is considered zero at the start and end points, that is, $\dot{x}_{p0} = \dot{y}_{p0} = \dot{x}_{pf} = \dot{y}_{pf} = 0$:

$$\begin{aligned}
&\textit{case } 1: \; x_1(0) = 0.1, \;\; x_2(0) = -0.3, \; x_1(t_f) = 0, \;\; x_2(t_f) = -0.22; \; t_f = 0.5 \text{ s} \\
&\textit{case } 2: \; x_1(0) = -0.1, \;\; x_2(0) = -0.3, \; x_1(t_f) = 0.05, \;\; x_2(t_f) = -0.25; \; t_f = 0.75 \text{ s} \\
&\textit{case } 3: \; x_1(0) = 0, \;\; x_2(0) = -0.24, \; x_1(t_f) = 0, \;\; x_2(t_f) = -0.34; \; t_f = 0.5 \text{ s} \\
&\textit{case } 4: \; x_1(0) = 0.075, \;\; x_2(0) = -0.28, \; x_1(t_f) = -0.075, \;\; x_2(t_f) = -0.28; \; t_f = 0.75 \text{ s}
\end{aligned} \tag{29}$$

By solving the TPBVP, the position and velocity of the end effector p and also the values of m_{c1}, m_{c2}, α_{c1}, and α_{c2} of the counterweights are obtained. Position of point p in case 2 for the forward and return motions is illustrated in Fig. 15. As seen in this figure, in the forward motion, point p moves from $[-0.1 \; -0.3]$ to $[0.05 \; -0.25]$. Then, in the return motion, point p returns from $[0.05 \; -0.25]$ to $[-0.1 \; -0.3]$.

https://doi.org/10.1017/S0263574720000971 Published online by Cambridge University Press

Table III. Optimal values of m_{c1}, m_{c2}, α_{c1}, and α_{c2} for different cases.

case	m_{c1} (g)	m_{c2} (g)	α_{c1} (deg)	α_{c2} (deg)
1	285.1065	500.9559	231.5737	124.8787
2	408.8644	359.3820	198.8428	158.0534
3	317.0116	317.0116	223.7515	136.2485
4	380.5313	380.5313	201.7857	158.2143

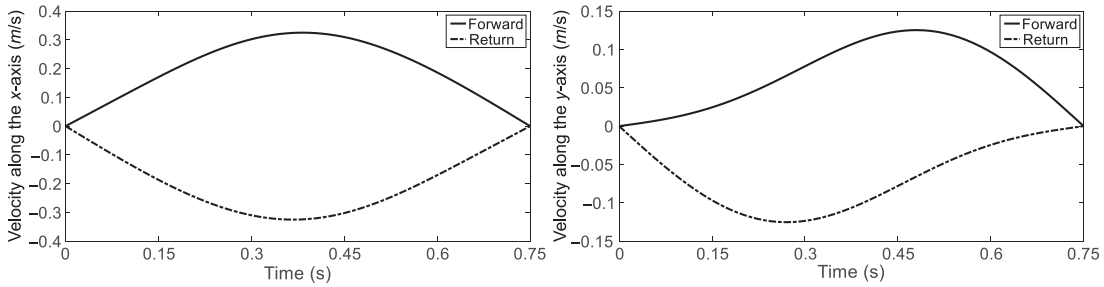

Fig. 16. Velocity of point p for case 2.

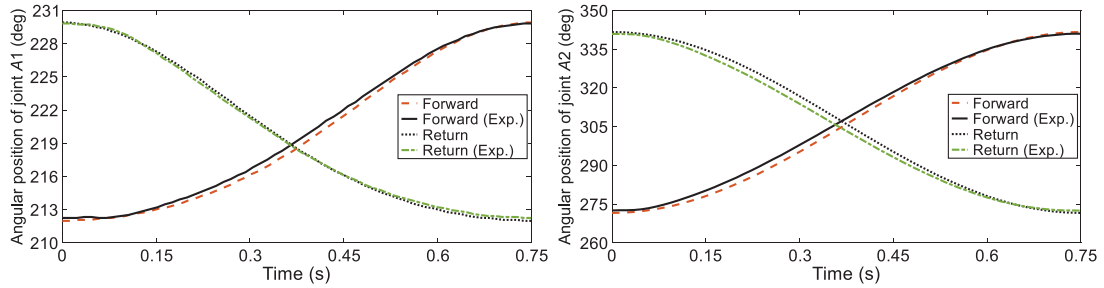

Fig. 17. Angular positions of active joints for case 2.
Exp.: Experimental.

The velocity of point p in case 2 for the forward and return motions is illustrated in Fig. 16. In the both forward and return motions, the zero velocity is expected at the both start and end points.

The optimal values of parameters m_{c1}, m_{c2}, α_{c1}, and α_{c2} of counterweights for different cases are given in Table III. For each case, the same values of parameters m_{c1}, m_{c2}, α_{c1}, and α_{c2} were obtained for the forward and return motions.

To compare the theoretical and experimental results, the angular position and velocity at the active joints are computed by Eqs. (2) and (3), respectively. The angular positions of the active joints A_1 and A_2 of the planar 5R parallel robot in case 2 for the forward and return motions are illustrated in Fig. 17 for the both numerical and experimental results. As seen in Fig. 17, the results of the TPBVP were in agreement with those of the experiment setup.

The angular velocities of the active joints in case 2 for the forward and return motions are illustrated in Fig. 18 for the both theoretical and experimental studies. The results of the TPBVP are in agreement with those of the experiments.

For case 2, the start and end positions of the planar 5R parallel robot with the counterweights are shown in Fig. 19. For the forward motion, the end effector of the robot moves from A to B. Next, in the return motion, the end effector of the robot moves from B to A.

For case 2, the trajectory of the robot end effector for the forward and return motions are shown in Fig. 20. This figure was obtained by taking a snapshot from the video file. The black curve shows the optimal trajectory of the end effector of the planar 5R parallel robot.

In order to record the end effector trajectory, a small red laser pointer is attached to the end effector. The end effector light path of the experiment setup was in agreement with the obtained optimal trajectory of the TPBVP. Note that the video was recorded from a rear view of the robot.

https://doi.org/10.1017/S0263574720000971 Published online by Cambridge University Press

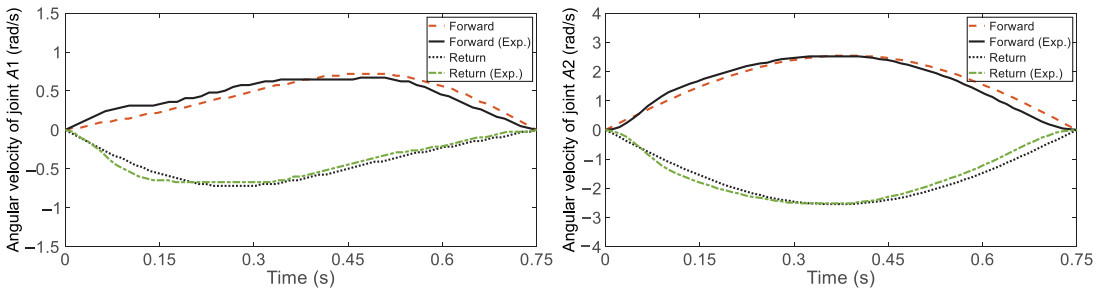

Fig. 18. Angular velocities of active joints for case 2.

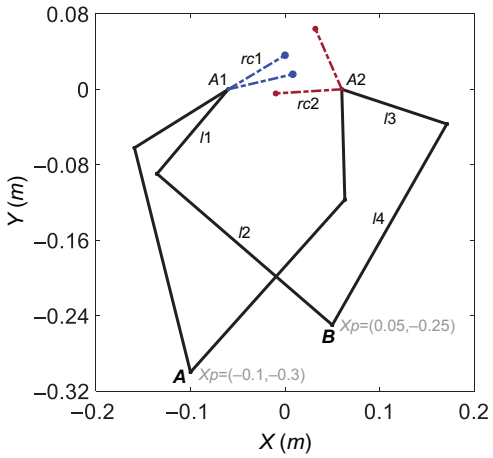

Fig. 19. Start and end points of robot in case 2.

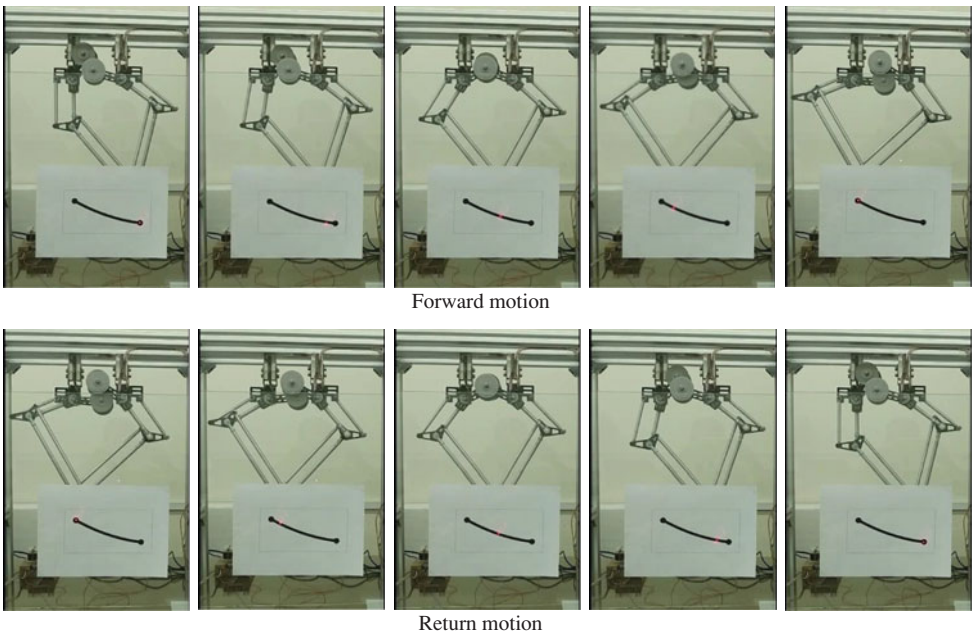

Fig. 20. Trajectory of end effector in case 2.

The numerically simulated and experimentally observed values of torque at active joints of the planar 5R parallel robot in case 2 are plotted in Fig. 21 for the forward and return motions.

As seen in Fig. 21, for the PTCM, the zero theoretical torque values were calculated for the forward and return motions. Also, by experimentally investigating the torque at active joints upon implementing the PTCM, the obtained values were considerably lower than those with TF condition.

https://doi.org/10.1017/S0263574720000971 Published online by Cambridge University Press

Table IV. Value of performance index.

Case	Condition		J((N.m)^2.s) Forward	Return	Average
1	TF	Theoretical	0.0609	0.0609	0.0609
		Experimental	0.0619	0.0617	0.0618
	Static balancing	Theoretical	0.0497	0.0498	0.0498
	PTCM	Theoretical	0	0	0
		Experimental	0.0059	0.0022	0.0040
2	TF	Theoretical	0.0819	0.0819	0.0819
		Experimental	0.0931	0.0912	0.0922
	Static balancing	Theoretical	0.0031	0.0032	0.0032
	PTCM	Theoretical	0	0	0
		Experimental	0.0063	0.0042	0.0052
3	TF	Theoretical	0.0440	0.0440	0.0440
		Experimental	0.0482	0.0474	0.0478
	Static balancing	Theoretical	0.0248	0.0251	0.0249
	PTCM	Theoretical	0	0	0
		Experimental	0.0045	0.0064	0.0055
4	TF	Theoretical	0.0794	0.0794	0.0794
		Experimental	0.0856	0.0849	0.0852
	Static balancing	Theoretical	0.0069	0.0069	0.0069
	PTCM	Theoretical	0	0	0
		Experimental	0.0058	0.0070	0.0064

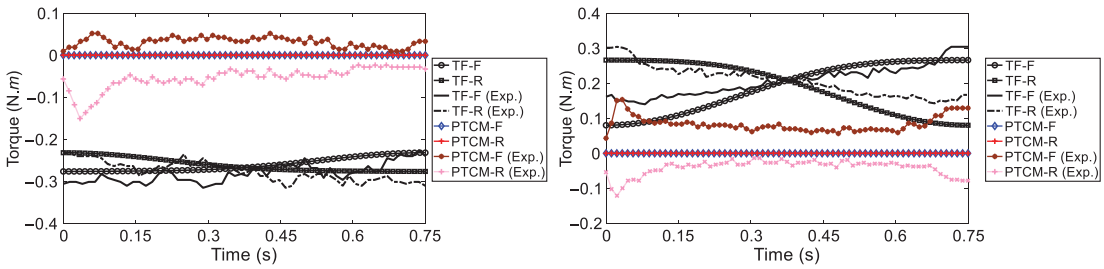

Fig. 21. Applied torque to joints A_1 (left) and A_2 (right) of robot – case 2.
F: Forward, R: Return, Exp.: Experimental.

Table IV presents the values of the performance index under different sets of condition according to Eq. (16). In the static balancing, the value of masses m_{c1}, m_{c2}, and m_{c3} are 1.4760, 0.2656, and 0.5629 kg, respectively, according to Eq. (11).

Based on the results presented in Table IV, the following conclusions can be drawn:

1. Theoretical simulation:

For the cases 1, 2, 3, and 4, the values of performance index with the TF condition were found to be 0.0609, 0.0819, 0.0440, and 0.0794, respectively. Under static balancing, the values of performance index for cases 1 to 4 are 0.0498, 0.0032, 0.0249, and 0.0069, respectively, while the corresponding values of the PTCM condition were all zero.

For the cases 1, 2, 3, and 4, the static balancing reduces the performance index respectively 18.23%, 96.09%, 43.41%, and 91.31%. The reduction of this index in the PTCM is 100%. As seen in the results, the efficiency of static balancing is decreased in high-speed motion.

https://doi.org/10.1017/S0263574720000971 Published online by Cambridge University Press

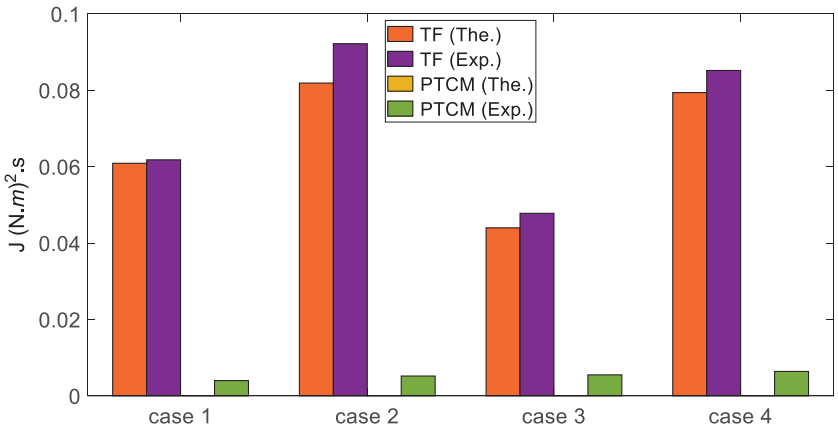

Fig. 22. Values of performance index for all cases.
The.: Theoretical, Exp.: Experimental.

2. Experimental implementation:

For the cases 1, 2, 3, and 4, the values of performance index with TF condition were calculated as 0.0618, 0.0922, 0.0478, and 0.0852, respectively, while the corresponding values for PTCM condition were 0.0040, 0.0052, 0.0055, and 0.0064, respectively.

In order to clarify the results given in Table IV, Fig. 22 presents the values of the performance index obtained from the theory and experimentation. The figure demonstrates the advantage of PTCM as compared with TF condition.

5. Conclusions

In this paper, PTCM was presented for a planar 5R parallel robot using optimal control problem formulation. The necessary conditions of PTCM for optimality of the robot were obtained by the PMP. In the PTCM, the states, torques at active joints, and unknown parameters of counterweights were determined simultaneously, ending up with zero performance index. The performance index is considered as the minimum effort. In the simulation study, it was shown that the required torques for the active joints can be omitted completely, and identical counterweights for the forward and return motions are calculated. Indeed, for a point-to-point motion, the values of m_{c1}, m_{c2}, α_{c1}, and α_{c2} of the counterweights were determined to obtain an optimal trajectory in which the robot can freely swing between the two desired points. For the purpose of validation, the optimal values of the counterweights were applied to a dynamic model of a planar 5R parallel robot created in the SimMechanics environment. The simulation results demonstrate the ability of the robot to oscillate freely between the initial and final positions without applying any torque. In order to demonstrate the effectiveness of the proposed method, an experiment setup was developed. In the practical implementation, significantly lower performance index values were obtained for the robot on which the PTCM was applied, as compared to the TF of the robot. According to experimental results, the performance index decreased by about 90% compared to the unbalanced robot.

Previous studies reduce the applied torques at joints, whereas the proposed method reduces the torque to zero. Compared to the static balancing method, it is a bit more difficult to implement. But the proposed method can be useful and economical for the high repetitive and high-speed motion. Indeed, the proposed method compensates the inertia force, gravity, Coriolis, and the centrifugal terms of the dynamic equation. Using the presented method, the maximum required torque and power of the actuators can be reduced considerably as shown in the experimental results. This aspect can reduce the actuator size of the robot in the design setup or increase the number of cycles per unit of time for an available robotic system. Although this method was successfully implemented for a point-to-point motion, it has a limitation in the industrial applications. The PTCM is not considered pause at the start and end points. However, a solution for the mentioned limit is the use of the servo motor which has a solenoid or electromagnetic brake.

https://doi.org/10.1017/S0263574720000971 Published online by Cambridge University Press

References

1. J. P. Merlet, *Parallel Robots* (Springer Science & Business Media, Netherlands, 2006).
2. H. Tourajizadeh and O. Gholami, "Optimal control and path planning of a 3PRS robot using indirect variation algorithm," *Robotica* **38**(5), 903–924 (2019).
3. T. Huang, Z. Li, M. Li, D. G. Chetwynd and C. M. Gosselin, "Conceptual design and dimensional synthesis of a novel 2-DOF translational parallel robot for pick-and-place operations," *J. Mech. Des.* **126**(3), 449–455 (2004).
4. F. Pierrot, S. Krut, C. Baradat and V. Nabat, "Par2: Aspatial mechanism for fast planar two-degree-of-freedom pick-and-place applications," *Meccanica* **46**(1), 239–248 (2011).
5. T. Huang, S. Liu, J. Mei and D. G. Chetwynd, "Optimal design of a 2-DOF pick-and-place parallel robot using dynamic performance indices and angular constraints," *Mech. Mach. Theory* **70**, 246–253 (2013).
6. Q. Meng, F. Xie and X. J. Liu, "V2: A Novel Two Degree-of-Freedom Parallel Manipulator Designed for Pick-and-Place Operations," *IEEE International Conference on Robotics and Biomimetics* (2017) pp. 1320–1327.
7. N. D. Sang, D. Matsuura, Y. Sugahara and Y. Takeda, "Kinematic Design of Five-Bar Parallel Robot by Kinematically Defined Performance Index for Energy Consumption," *European Conference on Mechanism Science* (2018) pp. 239–247.
8. U. Dincer and M. Cevik, "Improved trajectory planning of an industrial parallel mechanism by a composite polynomial consisting of Bezier curves and cubic polynomials," *Mecha. Mach. Theory* **132**, 248–263 (2019).
9. T. Chettibi, H. E. Lehtihet, M. Haddad and S. Hanchi, "Minimum cost trajectory planning for industrial robots," *Eur. J. Mech. A/Sol.* **23**(4), 703–715 (2004).
10. A. Gasparetto, P. Boscariol, A. Lanzutti and R. Vidoni, "Trajectory planning in robotics," *Math. Comput. Sci.* **6**(3), 269–279 (2012).
11. S. Lovlin, A. Abdullin, M. Tsvetkova and A. Mamatov, "Real-Time Optimal Trajectory Planning for Precision Tracking Systems with Dynamic Constraints," *26th International Workshop on Electric Drives: Improvement in Efficiency of Electric Drives* (IEEE, 2019) pp. 1–6.
12. L. P. Luo, C. Yuan, R. J. Yan, Q. Yuan, J. Wu, K. S. Shin and C. S. Han, "Trajectory planning for energy minimization of industry robotic manipulators using the Lagrange interpolation method," *Int. J. Precision Eng. Manuf.* **16**(5), 911–917 (2015).
13. P. Boscariol and A. Gasparetto, "Optimal trajectory planning for nonlinear systems: Robust and constrained solution," *Robotica* **34**(6), 1243–1259 (2016).
14. S. Kucuk, "Optimal trajectory generation algorithm for serial and parallel manipulators," *Robot. Comput. Integr. Manuf.* **48**, 219–232 (2017).
15. M. Bagheri and P. Naseradinmousavi, "Novel analytical and experimental trajectory optimization of a 7-DOF baxter robot: Global design sensitivity and step size analyses," *Int. J. Adv. Manuf. Tech.* **93**(9–12), 4153–4167 (2017).
16. S. Gong, R. Alqasemi and R. Dubey, "Gradient Optimization of Inverse Dynamics for Robotic Manipulator Motion Planning Using Combined Optimal Control," *ASME International Mechanical Engineering Congress and Exposition* (2017).
17. U. Nusbaum, M. W. Cohen and Y. Halevi, "Minimum Energy Control of Redundant Systems Using Evolutionary Bi-Level Optimization," *ASME International Mechanical Engineering Congress and Exposition* (2018).
18. J. Woolfrey, W. Lu and D. Liu, "A control method for joint torque minimization of redundant manipulators handling large external forces," *J. Intell. Robot. Syst.* **96**(1), 3–16 (2019).
19. P. Boscariol and D. Richiedei, "Energy-efficient design of multipoint trajectories for Cartesian robots," *Int. J. Adv. Manuf. Tech.* **102**(5–8), 1853–1870 (2019).
20. G. Quaglia and Z. Yin, "Static balancing of planar articulated robots," *Front. Mech. Eng.* **10**(4), 326–343 (2015).
21. A. Nikoobin and M. Moradi, "Optimal balancing of the robotic manipulators," **In:** *Dynamic Balancing of Mechanisms and Synthesizing of Parallel Robots* (Springer, 2016) pp. 337–363.
22. A. Nikoobin, M. R. Vezvari and M. Ahmadieh, "Optimal Balancing of Planar Cable Robot in Point to Point Motion Using the Indirect Approach," *3rd RSI International Conference on Robotics and Mechatronics* (IEEE, 2015) pp. 499–504.
23. M. R. Vezvari and A. Nikoobin, "Optimal balancing of spatial suspended cable robot in point-to-point motion using indirect approach," *Int. J. Adv. Des. Manuf. Tech.* **10**(3), 89–98 (2017).
24. V. Arakelian, "Gravity compensation in robotics," *Adv. Robot.* **30**(2), 79–96 (2016).
25. H. Misaghi, A. Mahmoudi and M. T. Masouleh, "Dynamic Analysis of a Planar Parallel Robot with the Purpose of Obtaining Optimal Inertial Parameters for Energy Consumption," *IEEE 4th International Conference on Knowledge-Based Engineering and Innovation* (2017) pp. 0931–0936.
26. M. Moradi, M. Naraghi and A. Kamali, "Simultaneous design of parameters and controller of robotic manipulators: Closed loop approach to practical implementation," *Adv. Robot.* **32**(3), 105–121 (2018).
27. A. Nikoobin and M. Moradi, "Analysis of optimal balancing for robotic manipulators in repetitive motions," *J. Dyn. Syst. Meas. Control* **140**(8), 1–8 (2018).
28. Y. Zhang, V. Arakelian and J. P. Le Baron, "Linkage Design for Gravity Balancing by Means of Non-zero Length Springs," **In:** *ROMANSY 22–Robot Design, Dynamics and Control* (Springer, Rennes, France, 2019) pp. 163–170.

https://doi.org/10.1017/S0263574720000971 Published online by Cambridge University Press

29. V. Gupta, S. K. Saha and H. Chaudhary, "Optimum design of serial robots," *J. Mech. Des.* **141**(8), 1–12 (2019).
30. A. Martini, M. Troncossi and A. Rivola, "Algorithm for the static balancing of serial and parallel mechanisms combining counterweights and springs: Generation, assessment and ranking of effective design variants," *Mech. Mach. Theory* **137**, 336–354 (2019).
31. D. Kirk, *An Introduction to Optimal Control Theory* (Prentice Hall, Englewood Cliffs, NI, 1970).
32. M. H. Korayem and A. Nikoobin, "Maximum payload for flexible joint manipulators in point-to-point task using optimal control approach," *Int. J. Adv. Manuf. Tech.* **38**(9–10), 1045–1060 (2008).
33. M. H. Korayem and A. Nikoobin, "Maximum payload path planning for redundant manipulator using indirect solution of optimal control problem," *Int. J. Adv. Manuf. Tech.* **44**(7–8), 725 (2009).
34. M. H. Korayem and H. Tourajizadeh, "Maximum DLCC of spatial cable robot for a predefined trajectory within the workspace using closed loop optimal control approach," *J. Intell. Robot. Syst.* **63**(1), 75–99 (2011).
35. M. H. Korayem, M. Nazemizadeh and H. N. Rahimi, "Trajectory optimization of nonholonomic mobile manipulators departing to a moving target amidst moving obstacles," *Acta Mechanica* **224**(5), 995–1008 (2013).
36. M. I. Rahaghi and F. Barat, "Solving nonlinear optimal path tracking problem using a new closed loop direct–indirect optimization method: Application on mechanical manipulators," *Robotica* **37**(1), 39–61 (2019).
37. X. J. Liu, J. Wang and G. Pritschow, "Kinematics, singularity and workspace of planar 5R symmetrical parallel mechanisms," *Mech. Mach. Theory* **41**(2), 145–169 (2006).
38. G. Alici and B. Shirinzadeh, "Optimum dynamic balancing of planar parallel manipulators based on sensitivity analysis," *Mech. Mach. Theory* **41**(12), 1520–1532 (2006).